Copper(II) Complexes of Novel N-Alkylated Derivatives of *cis,cis*-1,3,5-Triaminocyclohexane. 2. Metal-Promoted Phosphate Diester Hydrolysis

Kim A. Deal,[†] Gyungse Park,[‡] Junlong Shao,[‡] N. Dennis Chasteen,[‡] Martin W. Brechbiel,[†] and Roy P. Planalp*[,‡]

Radioimmune & Inorganic Chemistry Section, Radiation Oncology Branch, National Institutes of Health, Bethesda, Maryland 20892, and Department of Chemistry, University of New Hampshire, Durham, New Hampshire 03824

Received July 21, 2000

Aqueous copper(II) *N,N′,N″*-trimethyl-*cis,cis*-1,3,5-triaminocyclohexane (Cu(tach-Me_3)$^{2+}$(aq)) promotes the hydrolysis of activated phosphate diesters in aqueous medium at pH 7.2. This complex is selective for cleavage of the phosphate diester sodium bis(*p*-nitrophenyl) phosphate (BNPP), the rate of hydrolysis of the monoester disodium *p*-nitrophenyl phosphate being 1000 times slower. The observed rate acceleration of BNPP hydrolysis is slightly greater than that observed for other Cu(II) complexes, such as [Cu([9]aneN_3)Cl_2] ([9]aneN_3 ≡ 1,4,7-triazacyclononane). The rate of hydrolysis is first-order in phosphate ester at low ester concentration and second-order in [Cu(tach-Me_3)]$^{2+}$(aq), suggesting the involvement of two metal complexes in the mechanism of substrate hydrolysis. The reaction exhibits saturation kinetics with respect to BNPP concentration according to a modified Michaelis−Menten mechanism: 2CuL + S ⇌ LCu−S−CuL → 2CuL + products (K_M = 12.3 ± 1.8 mM^2, k_{cat} = (4.0 ± 0.4) × 10^{-4} s^{-1}, 50 °C) where CuL ≡ [Cu(tach-Me_3)]$^{2+}$, S ≡ BNPP, and LCu−S−CuL is a substrate-bridged dinuclear complex. EPR data indicate that the dicopper complex is formed only in the presence of BNPP; the active LCu−S−CuL intermediate species then slowly decays to products, regenerating monomeric CuL.

Introduction

Nature has developed nucleases to hydrolyze phosphate diester bonds, which are components of exceptionally stable compounds responsible for the accuracy of the genetic code. There has been considerable interest in the development of inorganic complexes that function as synthetic metallonucleases.[1−5] A variety of inert metal compounds have been evaluated as promoters (or catalysts) of activated phosphate diester hydrolysis.[6−11] Recently, efforts have focused on complexes of labile metals,[12−16] including Zn(II), Cu(II), and the lanthanides, in analogy to the active sites of natural nucleases, which often contain one or two labile metal cations in the active site.[17−19]

One of the first Cu(II) systems evaluated, Cu(2,2′-bipyridine)$^{2+}$, catalyzed the hydrolysis of ethyl *p*-nitrophenyl phosphate.[20] Since then, others have explored Cu(II) complexes of 2,2′-bipyridine and pyridine derivatives in similar reactions.[21−23] A variety of activated phosphate diesters and activated transesterification substrates, such as bis(2,4-dinitrophenyl) phosphate,[23] bis(*p*-nitrophenyl) phosphate (BNPP),[21,22] and 2-hydroxypropyl *p*-nitrophenyl phosphate (HPNP)[24,25] have been used to demonstrate the activity of Cu(II) complexes.

Mechanistic study of Cu(II)-catalyzed phosphate diester hydrolysis has yielded a variety of kinetic behaviors and proposed active species. The Cu(II) triaza-macrocycle systems ([Cu([*n*]aneN_3)Cl_2], *n* = 9, 10, 11) have been investigated in detail.[26,27] The authors measured a half-order rate dependence in metal complex, which was attributed to the formation of

* Corresponding author. Phone: (603) 862-2471. Fax: (603) 862-4278. E-mail: roy.planalp@unh.edu.
[†] National Institutes of Health.
[‡] University of New Hampshire.

(1) Hegg, E.; Burstyn, J. *Coord. Chem. Rev.* **1998**, *173*, 133−165.
(2) Bashkin, J. *Curr. Biol.* **1997**, *7*, R286−R288.
(3) Morrow, J. *Metal Ions Biol. Syst.* **1996**, *33*, 561−592.
(4) Sigman, D.; Mazumder, A.; Perrin, D. *Chem. Rev.* **1993**, *93*, 2295−2316.
(5) Kuusela, S.; Lönnberg, H. *Metal Ions Biol. Syst.* **1996**, *32*, 271−300.
(6) Wahnon, D.; Lebuis, A.; Chin, J. *Angew. Chem., Int. Ed. Engl.* **1995**, *34*, 2412−2414.
(7) Williams, N.; Cheung, W.; Chin, J. *J. Am. Chem. Soc.* **1998**, *120*, 8079−8087.
(8) Hendry, P.; Sargeson, A. *Prog. Inorg. Chem.* **1990**, *38*, 201−258.
(9) Hendry, P.; Sargeson, A. *Inorg. Chem.* **1990**, *29*, 92−97.
(10) Hendry, P.; Sargeson, A. *J. Am. Chem. Soc.* **1989**, *111*, 2521−2527.
(11) Chin, J.; Banaszczyk, M.; Jubian, V.; Zou, X. *J. Am. Chem. Soc.* **1989**, *111*, 186−190.
(12) Yashiro, M.; Ishikubo, A.; Komiyama, M. *J. Chem. Soc., Chem. Commun.* **1995**, 1793−1794.
(13) Yashiro, M.; Ishikubo, A.; Komiyama, M. *J. Chem. Soc., Chem. Commun.* **1997**, 83−84.
(14) Gobel, M. *Angew. Chem., Int. Ed. Engl.* **1994**, *33*, 1141−1143.
(15) Koike, T.; Kimura, E. *J. Am. Chem. Soc.* **1991**, *113*, 8935−8941.
(16) De Rosch, M.; Trogler, W. C. *Inorg. Chem.* **1990**, *29*, 2409−2416.
(17) Williams, N. In *Comprehensive Biological Catalysis*; Sinnot, M., Ed.; Academic Press: San Diego, CA, 1998; Vol. I, pp 543−561.
(18) Cowan, J. *Chem. Rev.* **1998**, *98*, 1067−1087.
(19) Sträter, N.; Lipscomb, W.; Klabunde, T.; Krebs, B. *Angew. Chem., Int. Ed. Engl.* **1996**, *35*, 2024−2055.
(20) Morrow, J.; Trogler, W. *Inorg. Chem.* **1988**, *27*, 3387−3394.
(21) Kovari, E.; Heitker, J.; Kramer, R. *J. Chem. Soc., Chem. Commun.* **1995**, 1205−1206.
(22) Kovari, E.; Krämer, R. *J. Am. Chem. Soc.* **1996**, *118*, 12704−12709.
(23) Young, M.; Wahnon, D.; Hynes, R.; Chin, J. *J. Am. Chem. Soc.* **1995**, *117*, 9441−9447.
(24) Wall, M.; Hynes, R.; Chin, J. *Angew. Chem., Int. Ed. Engl.* **1993**, *32*, 1633−1635.
(25) Wahnon, D.; Hynes, R.; Chin, J. *J. Chem. Soc., Chem. Commun.* **1994**, 1441−1442.
(26) Deal, K.; Burstyn, J. *Inorg. Chem.* **1996**, *35*, 2792−2798.
(27) Hegg, E.; Mortimore, S.; Cheung, C.; Huyett, J.; Powell, D.; Burstyn, J. *Inorg. Chem.* **1999**, *38*, 2961−2968.

10.1021/ic000830d CCC: $20.00 © 2001 American Chemical Society
Published on Web 07/07/2001

Scheme 1

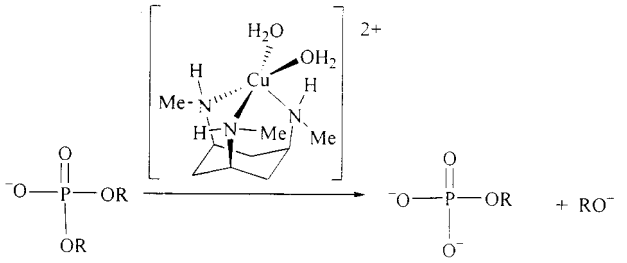

inactive dihydroxo-bridged copper(II) dimers $[Cu([n]aneN_3)(OH)]_2^{2+}$ in equilibrium with the direct catalyst precursors, $[Cu([n]aneN_3)(OH)]^+$.[26,28] Thus, the monomers $[Cu([n]aneN_3)(OH)]^+$ were proposed to be active because they possess an available hydroxide ion as nucleophile for diester cleavage. Differences in hydrolysis rate among the $[n]aneN_3$ ligands were attributed to steric effects that could favor a dimer for the complexes with smaller *n*, whose hydroxide is unavailable.[27] In contrast, a first-order metal dependence on the $Cu([12]aneN_3)^{2+}$ complex, formed in situ, in the hydrolysis of ethyl 2,4-dinitrophenyl phosphate was reported.[29] Wahnon and co-workers[25] noted the transesterification rate of HPNP by the Cu(II) complex of tridentate bis(2-benzimidazolylmethyl)amine had a second-order dependence on metal complex concentration, which was ascribed to an active monohydroxo-bridged dimer. The steric bulk of this amine ligand may inhibit formation of the inactive dihydroxo-bridged copper(II) dimer.

We have initiated a study of Cu(II) complexes of *N*,*N*′,*N*″-trialkylated derivatives of *cis*,*cis*-1,3,5-triaminocyclohexane (designated $[Cu(tach\text{-}R_3)Cl_2]$), based on the observations that tridentate amines whose steric bulk may be regulated could lead to further understanding of mechanism of phosphate diester cleavage by Cu(II) (Scheme 1).[30] Until recently, the availability of tach, and therefore its derivatives, was limited by available syntheses. We have developed a high-yield synthesis of tach[31] and exploited this to prepare a new family of trialkyl derivatives, tach-R_3 (R = Me, Et, *n*-Pr, CH_2-2-thienyl, and CH_2-2-furanyl) and 2-pyridylmethyl hexadentate derivatives, $(N-R)_3$tachpyr.[31,32] Tach-based hexadentate ligands form complexes with a variety of metal ions, including Fe(II),[32] Cu(II),[30,33] Zn(II), Cd(II), Hg(II),[34] Ga(III), and In(III).[35] The structural and electronic properties of the $Cu^{II}(tach\text{-}R_3)$ complexes are reported in the preceding paper;[33] the speciation of the aqueous Cu(II)−tach-R_3 complexes is believed to be $[Cu(tach\text{-}R_3)(H_2O)_2]^{2+}$, referred to as "$Cu(tach\text{-}R_3)^{2+}$" herein. As this study began, Fujii and co-workers[29,36] reported that the rate of hydrolysis of ethyl 2,4-dinitrophenyl phosphate by the Cu(II) complex of unalkylated *cis*,*cis*-1,3,5-triaminocyclohexane ($Cu(tach\text{-}H_3)^{2+}$) was significantly greater than that of Cu(II) complexes of several other triamine ligands. Here we report the hydrolysis of activated phosphate diesters such as bis(*p*-nitrophenyl) phosphate (BNPP) at neutral pH by $Cu(tach\text{-}Me_3)^{2+}$(aq) (Scheme 1, R = *p*-nitrophenyl). A kinetic study and proposed mechanism of action are described.

Experimental Section

The buffer HEPES (*N*-(2-hydroxyethyl)piperazine-*N*′-ethanesulfonic acid) was purchased from Sigma Chemical Co. Sodium bis(*p*-nitrophenyl) phosphate (BNPP), sodium ethyl *p*-nitrophenyl phosphate, disodium *p*-nitrophenyl phosphate, $Na_4P_4O_7 \cdot 10H_2O$, $CuSO_4 \cdot 5H_2O$, $CuCl_2$ (anhydrous), triethylamine, and sodium perchlorate were purchased from Aldrich.

^{63}Cu metal was obtained from Cambridge Isotope Laboratories. Sodium hydroxide and acetic acid were purchased from Mallinckrodt Chemical, and HPLC grade methanol was purchased from J. T. Baker. Triethylamine was distilled from CaH_2 before use, and all other chemicals were used without further purification. Aqueous solutions were prepared with water purified by passage through a Hydro ultrapure water filtration system.

An Accumet pH Meter 925 equipped with an Orion 8103 Ross semimicro combination pH electrode was used for pH measurements. Quartz cuvettes with threaded caps were obtained from Hellma. HPLC analysis was performed on a Beckman system with a variable wavelength detector interfaced with a PC. Separations were obtained on a Beckman Ultrasphere ODS C-18 reversed-phase column (4.6 mm × 25 cm).

***In Situ* Preparation of (*N*,*N*′,*N*″-Trimethyl-*cis*,*cis*-1,3,5-triaminocyclohexane)copper(II).** *N*,*N*′,*N*″-Trimethyl-*cis*,*cis*-1,3,5-triaminocyclohexane trihydrobromide salt (tach-$Me_3 \cdot 3HBr$) was prepared by the literature method.[15,16] Aqueous $CuCl_2$ (1.49 mL, 0.1 M) was added to aqueous tach-$Me_3 \cdot 3HBr$ (1.5 mL, 0.1 M, neutralized with 3 equiv of NaOH) to afford a deep blue solution of $Cu(tach\text{-}Me_3)^{2+}$ (50 mM) that was used without further purification. Occasionally, a faint blue-green precipitate formed, presumably insoluble Cu(II) hydroxides, which was removed by filtration through a 0.22 μm syringe filter.

Product Analysis. HEPES (2.64 mL of 50 mM aqueous, pH 7.2 standardized at 50 °C), $Cu(tach\text{-}Me_3)^{2+}$ (60 μL of 50 mM aqueous), and BNPP (300 μL of 10 mM aqueous) were combined giving final concentrations of 1.0 mM BNPP and 1.0 mM $Cu(tach\text{-}Me_3)^{2+}$ in 3.00 mL total volume of HEPES (44 mM). The solution was incubated at 50 °C for 1 h. An aliquot was withdrawn and analyzed by reversed-phase HPLC, eluted with a linear gradient of 100% 50 mM acetic acid/50 mM triethylamine to 100% methanol over 25 min. The products were equal amounts of *p*-nitrophenol and *p*-nitrophenyl phosphate, as confirmed by co-injection of standard 1 mM solutions of *p*-nitrophenol, *p*-nitrophenyl phosphate, and BNPP (retention times of 16.8, 10.5, and 20.2 min, respectively).

Kinetics. The studies were based on previously published work.[26] The method of initial rates was used, whereby reaction progress was monitored spectrophotometrically in situ in Teflon-sealed screw-capped quartz cuvettes in an HP 8450A diode array UV/vis spectrometer, fitted with a water-jacketed multicell holder and interfaced to an IBM PC. The temperature of the multicell holder was maintained at 50 °C with a Forma Scientific circulating bath. Aliquots of stock solutions of $Cu(tach\text{-}Me_3)^{2+}$ (typically 50 mM) and substrate (e.g., BNPP, typically 10−20 mM) were added to an appropriate volume of HEPES (50 mM, pH 7.2 at 50 °C) to provide a total reaction volume of 3 mL.

The progress of the reaction was indicated by the absorbance at 400 nm, assigned to *p*-nitrophenolate (ϵ = 18 700 L mol^{-1} cm^{-1}).[27] To account for the fraction of *p*-nitrophenolate that exists as its conjugate acid at pH 7.2,[26] the pK_a's of HEPES buffer (apparent pK_a' = 7.31, 37 °C, I = 0.1 M)[37] and of *p*-nitrophenol (thermodynamic pK_a = 7.15, 25 °C, I = 0)[38] were corrected to the apparent values appropriate for the temperature and ionic strength of our experiments (50 °C, $I \sim 45$ mM),

(28) Burstyn, J. N.; Deal, K. A. *Inorg. Chem.* **1993**, *32*, 3585−3586.
(29) Itoh, T.; Hisada, H.; Usui, Y.; Fujii, Y. *Inorg. Chim. Acta* **1998**, *283*, 51−60.
(30) Ye, N.; Rogers, R. D.; Brechbiel, M. W.; Planalp, R. P. *Polyhedron* **1998**, *17*, 603−606.
(31) Bowen, T.; Planalp, R. P.; Brechbiel, M. W. *Bioorg. Med. Chem. Lett.* **1996**, *6*, 807−810.
(32) Park, G.; Lu, F.; Ye, N.; Brechbiel, M.; Torti, S.; Torti, F.; Planalp, R. *JBIC* **1998**, *3*, 449−457.
(33) Park, G.; Lu, F. H.; Shao, J.; Chasteen, N. D.; Rogers, R. D.; Brechbiel, M. W.; Planalp, R. P. *Inorg. Chem.* **2001**, 4167.
(34) Park, G.; Ye, N.; Rogers, R.; Brechbiel, M.; Planalp, R. *Polyhedron* **2000**, *19*, 1155−1161.
(35) Hilfiker, K. A.; Rogers, R. D.; Brechbiel, M. W.; Planalp, R. P. *Inorg. Chem.* **1997**, *36*, 4600−4603.
(36) Itoh, T.; Hisada, H.; Sumiya, T.; Hosono, M.; Usui, Y.; Fujii, Y. *J. Chem. Soc., Chem. Commun.* **1997**, 677−678.
(37) Good, N.; Winget, G.; Winter, W.; Connelly, T.; Izana, S.; Singh, R. *Biochemistry* **1966**, *5*, 467−477.
(38) Martell, A.; Smith, R. *Critical Stability Constants*; Plenum Press: New York, 1977; Vol. 3, p 183.

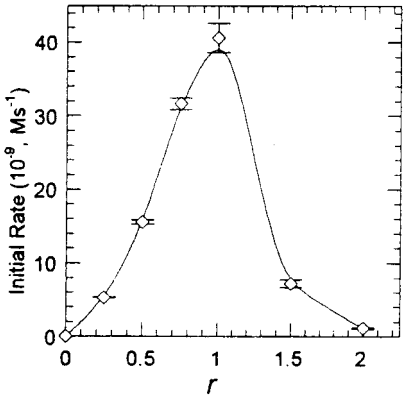

Figure 1. Effect of the Cu^{2+} to ligand ratio (r) on the initial rate of hydrolysis of bis(*p*-nitrophenyl) phosphate. Reaction solutions were prepared from 0.1 M stock solutions of $CuCl_2$ and tach-Me_3. Each reaction mixture contained 50 mM HEPES, pH 7.2, at $T = 50$ °C and 5 mM bis(*p*-nitrophenyl) phosphate. The final concentrations of Cu^{2+} varied from 2.1×10^{-4} to 8.3×10^{-4} M, and those of tach-Me_3 varied from 8.3×10^{-4} to 4.2×10^{-4} M. Error bars are shown on the graph and may be within the data point.

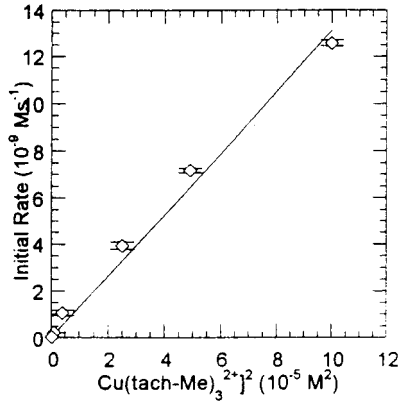

Figure 2. Plot of initial rate versus $[Cu(tach\text{-}Me_3)^{2+}]^2$ of hydrolysis of bis(*p*-nitrophenyl) phosphate. Each reaction mixture contained 50 mM HEPES, pH 7.2, at 50 °C and 0.1 mM bis(*p*-nitrophenyl) phosphate. The concentration of $Cu(tach\text{-}Me_3)^{2+}$ was varied from 0.5 to 10 mM. Error bars are within the data point, and the plotted line is the computer-generated best fit with $R = 0.9958$.

giving $pK_a' = 7.20$ (HEPES) and $pK_a' = 6.71$ (*p*-nitrophenol). Activity coefficients were computed from the Davies equation with $A = 0.524$ mol$^{-1/2}$ kg$^{1/2}$ for 50 °C[39,40] and included a 10% contribution of the zwitterionic form of HEPES to log $\gamma_{\pm}$[40] as well as ionic strength contributions from the dissociated HEPES, $Cu(tach\text{-}Me_3)Cl_2$, and BNPP. Corrections to the pK_a for temperature were made using the temperature coefficient $\Delta pK_a'/\Delta T = -0.014$ of HEPES[37] and using the enthalpy of ionization $\Delta H° = 4.5$ kcal/mol for *p*-nitrophenol[38] and the van't Hoff equation. Under the conditions of our experiments 29.6 ± 1.5% of the *p*-nitrophenol exists as its conjugate acid. Therefore, after interpretation of the absorbances with the cited $\epsilon = 18\,700$ L mol^{-1} cm^{-1}, the determined rates were corrected by a factor of 1.40. The absorbance of $Cu(tach\text{-}Me_3)^{2+}$ ($\lambda_{max} = 664$ nm, $\epsilon = 109$ L mol^{-1} cm^{-1}) did not interfere in the determination of *p*-nitrophenolate.

The increase in absorbance at 400 nm was followed for 60 min, which represented less than 15% conversion of bis(*p*-nitrophenyl) phosphate to products. All runs were conducted in triplicate, from which standard deviations of typically 1−5% were obtained, as indicated by error bars in the data plots (Figures 1−3 and 5). The sample in the reference beam was identical to the reaction mixture, except lacking metal complex, thereby correcting for possible uncatalyzed hydrolysis of the phosphate diester. Control experiments (below) were also conducted to examine other sources of hydrolysis.

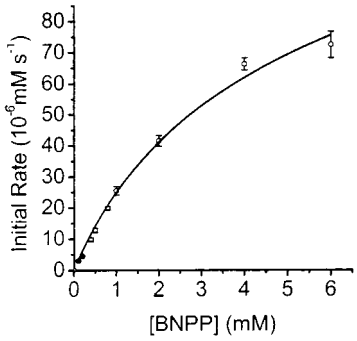

Figure 3. Saturation kinetics of $Cu(tach\text{-}Me_3)^{2+}$ by bis(*p*-nitrophenyl) phosphate. Each reaction mixture contained 50 mM HEPES, pH 7.2, at 50 °C and 1 mM $Cu(tach\text{-}Me_3)^{2+}$. The concentration of bis(*p*-nitrophenyl) phosphate was varied from 0.2 to 6 mM. Error bars are shown on the graph and may be within the data point. The plotted line is the computer-generated best fit according to eq 7 where $K_M = 12.3 \pm 1.8$ mM^2 and $k_{cat} = (4.0 \pm 0.4) \times 10^{-4}$ s^{-1}.

Two control experiments were conducted to ensure that the hydrolysis observed during the kinetics measurements was due to the copper complex. To examine possible background hydrolysis of BNPP in the buffer medium, HEPES (2.70 mL of 50 mM aqueous, pH 7.2 at 50 °C) and BNPP (300 μL of 10 mM aqueous) were combined giving a final concentration of 1 mM BNPP in 3 mL total volume of HEPES (45 mM). This solution was incubated at 50 °C for 1 h while monitoring the *p*-nitrophenolate absorbance at 400 nm. The possibility of hydrolysis of BNPP by the free chelator (tach-Me_3) was examined by a similar procedure. HEPES (5.10 mL of 50 mM aqueous, pH 7.2), tach-Me_3·3HBr (300 μL of 10 mM aqueous), and BNPP (300 μL of 10 mM aqueous) were combined giving final concentrations of 0.5 mM BNPP and 0.5 mM tach-Me_3 in 5.7 mL total volume of HEPES (44.7 mM). In both cases, no appearance of *p*-nitrophenolate was detected over a period of 1 h.

The procedure for measurement of the reaction rate dependence on concentration of $Cu(tach\text{-}Me_3)^{2+}$ (Figure 2) is typical of the methods employed. In six experiments (each conducted in triplicate), aliquots of $Cu(tach\text{-}Me_3)^{2+}$ (50 mM) ranging in volume from 23 to 600 μL were added to 2.94 to 2.37 mL of HEPES buffer (50 mM) to produce final concentrations of $Cu(tach\text{-}Me_3)^{2+}$ ranging from 0.5 mM to 10 mM. BNPP (30 μL, 10 mM) was added to each run to give a final [BNPP] of 0.1 mM, in 3 mL total volume of HEPES (39.5−49 mM, respectively). The progress of the reaction was monitored spectrophotometrically at 400 nm. The absorbance data was processed by Kaleidagraph (Synergy Software) to give the initial rate plots. Curve fitting of the saturation kinetics was done with Origin 6.0 (Microcal).

Preparation of $^{63}Cu(tach\text{-}Me_3)^{2+}$. To a clear solution of tach-Me_3·3HBr (0.0021 g, 5.0×10^{-6} mol) in 0.25 mL of a 2:1 v/v mixture of 50 mM HEPES (pH 7.4 in D_2O) and glycerol-d_3 was added a pale blue solution of 20 mM $^{63}CuCl_2$ (0.25 mL, 5.0×10^{-6} mol) in DCl (0.01 M) affording a blue solution of 10 mM $^{63}Cu(tach\text{-}Me_3)^{2+}$. From this was prepared 1 mM $^{63}Cu(tach\text{-}Me_3)^{2+}$ by further dilution with the 50 mM HEPES/glycerol-d_3 mixture.

Reaction Mixture of $Cu(tach\text{-}Me_3)^{2+}$ and BNPP for EPR Study. Aqueous $Cu(tach\text{-}Me_3)^{2+}$ (40 μL, 50 mM) and BNPP (1 mL, 20 mM in 50 mM HEPES) were added to HEPES (960 μL, 50 mM) to provide final concentrations of 1 mM $Cu(tach\text{-}Me_3)^{2+}$ and 10 mM BNPP in a total volume of 2 mL of HEPES (49 mM).

EPR Measurements. The EPR spectra were measured on a laboratory-assembled X-band spectrometer equipped with a Bruker ER 041 XK-H microwave bridge and a Varian TE_{102} cavity as described elsewhere.[41] Calibrated 3 mm i.d.−4 mm o.d. quartz sample tubes were used for measurements on frozen solutions at 77 K. A quartz flat cell was used for room-temperature measurements on aqueous solutions.

(39) Klotz, I.; Rosenberg, R. *Chemical Thermodynamics*; John Wiley and Sons: New York, 1994; p 438.
(40) Perrin, D.; Dempsey, B. *Buffers for pH and Metal Ion Control*; Chapman and Hall: London, 1974; pp 6−10.
(41) Yang, X.; Chasteen, N. D. *Biophys. J.* **1996**, *71*, 1587−1595.

Chart 1

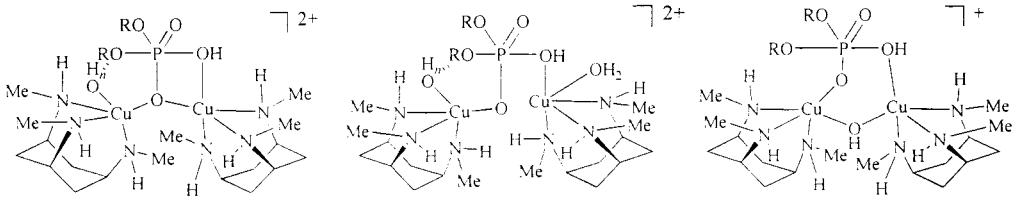

1a, n = 1 or 2 **1b**, n = 1 or 2 **1c**

The EPR spectra of frozen solution samples at 77 K were collected at relatively low microwave power to avoid signal saturation. About 400 μL volume of sample was added to either the quartz tubes or to the flat cell. For measurements at 77 K, the samples were frozen immediately after preparation. A solution of 1 mM $CuSO_4$ in 1:3 glycerol:water, pH 2, served as an absolute intensity standard for frozen solution spectra. The spectrometer settings for frozen solutions were the following: microwave power = 5 mW; modulation amplitude = 0.2 mT at 100 kHz; scan time = 500 s; time constant = 0.3 s; frequency = 9.1500 GHz; scan range = 100 mT. Room-temperature spectra were obtained with the following settings: microwave power = 10 mW; modulation amplitude = 0.5 mT; scan time = 1000 s; time constant = 1 s; scan range = 100 mT; frequency = 9.5284 GHz. To maximize the cavity Q, the orientation and tilt of the flat cell were carefully adjusted by observing the cavity tuning mode on the oscilloscope. Reproducibility in the EPR signal intensity between tunings of the spectrometer on the same sample was ±1.0%.

Results

Cu(tach-Me_3)$^{2+}$ and Products of Phosphate Diester Cleavage. A solution of Cu(tach-Me_3)$^{2+}$ was prepared either by dissolving an appropriate quantity of solid [Cu(tach-Me_3)Cl_2] in HEPES buffer or by generating the material in situ (Experimental Section). In the preceding article, it has been shown through EPR studies that the solution species generated by these two methods are equivalent.[33] The in situ method was used in these studies because high concentrations of Cu(tach-Me_3)$^{2+}$ could be quickly and efficiently generated. It has also been shown that [Cu(tach-Et_3)Cl_2] undergoes rapid hydrolysis of Cu−Cl bonds to give an aquo species, formulated as [Cu(tach-Et_3)-$(H_2O)_2$]$^{2+}$, with a square-pyramidal structure and a nitrogen donor in the apical position.[33] Thus, aqueous Cu(tach-Me_3)$^{2+}$ is reasonably presumed to have a similar structure, as depicted in Scheme 1. The products of phosphate diester cleavage shown in Scheme 1 were determined by reversed-phase HPLC with UV detection to be *p*-nitrophenol and *p*-nitrophenyl phosphate formed in equal amounts (Experimental Section). The nature of the products and the absence of other UV-active peaks suggest a hydrolytic mechanism of cleavage.

Kinetic Analysis. Kinetics of the reaction between Cu(tach-Me_3)$^{2+}$ and bis(*p*-nitrophenyl) phosphate were studied by the method of initial rates. The method of initial rates is a convenient method for collecting kinetic data for slow reactions, because only 5−10% completion is necessary. Copper(II) complex-promoted hydrolysis of phosphate diesters is generally a slow reaction,[20,26,28] which is not practical to follow for 3−5 half-lives. The reaction was followed spectrophotometrically, and the only significant spectral change occurred at 400 nm, which corresponds to the production of the *p*-nitrophenolate anion. No detectible BNPP hydrolysis was observed in absence of copper complex or with tach-Me_3 alone under otherwise identical reaction conditions.

Because Cu(tach-Me_3)$^{2+}$ was generated in situ, with the possible existence of various species of different Cu:L stoichiometry, studies were performed to determine the [Cu(II)]:[(tach-Me_3)] ratio (r) which yielded the greatest hydrolytic rate. As shown in Figure 1, the maximum rate was obtained at equal concentrations of Cu(II) and tach-Me_3. As r exceeded one, the decline in rate was accompanied by precipitation of uncharacterized blue salts.

The hydrolysis of bis(*p*-nitrophenyl) phosphate by Cu(tach-Me_3)$^{2+}$ exhibited second-order dependence with respect to the metal complex. A plot of the initial rate versus the concentration of Cu(tach-Me_3)$^{2+}$ squared was linear with a slope of 1.3×10^{-4} M^{-1} s^{-1} (R = 0.996) (Figure 2). The reaction order with respect to bis(*p*-nitrophenyl) phosphate was also determined. The rate of hydrolysis of the phosphate diester is first-order in BNPP at low substrate concentration but becomes saturated at higher concentrations relative to that of Cu(tach-Me_3)$^{2+}$ (Figure 3), consistent with a mechanism whereby Cu(tach-Me_3)$^{2+}$ forms a reasonably strong complex with the substrate BNPP prior to hydrolysis.

Mechanistic Analysis. The following mechanism (eqs 1−3) is consistent with the observed reaction orders and saturation kinetics. The previously described aqua Cu(tach-Me_3)$^{2+}$ complex[33] is denoted by LCu and substrate (BNPP) by S:

$$\mathrm{CuL} + \mathrm{S} \overset{K_1}{\rightleftharpoons} \mathrm{LCu{-}S} \quad (1)$$

$$\mathrm{LCu} + \mathrm{LCu{-}S} \overset{K_2}{\rightleftharpoons} \mathrm{LCu{-}S{-}CuL} \quad (2)$$

$$\underset{\mathbf{1a-c}}{\mathrm{LCu{-}S{-}CuL}} \xrightarrow{k_{cat}} 2\mathrm{CuL} + \mathrm{products} \quad (3)$$

The intermediate LCu−S−CuL is postulated to have one of the three structures **1a**−**c** as shown in Chart 1.

We assume that steps 1 and 2 of the mechanism are in preequilibrium and the slow-hydrolysis step 3 is rate-limiting. It follows that the equilibrium concentration of intermediate is given by eq 4 and the rate of product formation by eq 5:

$$[\mathrm{LCu{-}S{-}CuL}] = K_1K_2[\mathrm{LCu}]^2[\mathrm{S}] \quad (4)$$

$$\mathrm{d[products]/dt} = \mathrm{k_{cat}[LCu{-}S{-}CuL]} = \mathrm{k_{cat}}K_1K_2[\mathrm{LCu}]^2[\mathrm{S}] \quad (5)$$

Equation 5 is in accord with the observed order of the reaction. Since the equilibrium concentration of LCu−S−CuL governs the rate of the reaction, we write the mechanism in condensed form as a modified Michaelis−Menten mechanism:

$$2\mathrm{CuL} + \mathrm{S} \overset{K_1K_2}{\rightleftharpoons} \mathrm{LCu{-}S{-}CuL} \xrightarrow{k_{cat}} 2\mathrm{CuL} + \mathrm{products} \quad (6)$$

Saturation kinetics is expected when a significant fraction of the total copper is present as the intermediate LCu−S−CuL, the concentration of which is given by eq 4. To express the kinetics in terms of the total concentrations of CuL and S in solution, we write the mass balance equations $[\mathrm{CuL}]_o = [\mathrm{CuL}]$

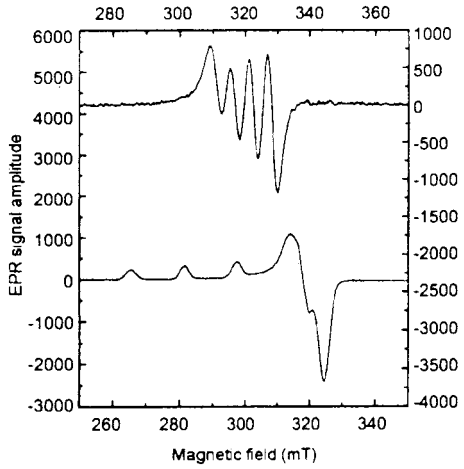

Figure 4. X-band EPR spectra of Cu(tach-Me_3)$^{2+}$ in room temperature (a) and frozen (b) solution. See Experimental Section for spectrometer settings.

$+ 2[LCu-S-CuL]$ and $[S]_o = [S] + [LCu-S-CuL] \approx [S]$ because the substrate concentration, [S], is in excess. By combining these equations with eqs 4 and 5, we derive the following expression for the dependence of the initial rate v_o of the reaction on the total substrate concentration $[S]_o$ at a fixed total copper concentration $[CuL]_o$:

$$v_o = k_{cat}K_M\{4[CuL]_o[S]_o/K_M + 1 - (8[CuL]_o[S]_o/K_M + 1)^{1/2}\}/8[S]_o \quad (7)$$

For preequilibrium the Michaelis constant is defined as $K_M = 1/(K_1K_2)$ and is an overall dissociation constant for the intermediate. In this analysis, K_M corresponds to the product of total concentrations, $[CuL]_o[S]_o$, that produces an initial rate that is half its maximal value. The maximal velocity of the reaction under conditions of substrate saturation is given by $v_{max} = k_{cat}[CuL]_o/2$. The factor of 2 arises from the fact that two copper complexes are involved in formation of the intermediate. Figure 3 shows the rate data fitted to eq 7, from which we obtain $K_M = 12.3 \pm 1.8$ mM^2 and $k_{cat} = (4.0 \pm 0.4) \times 10^{-4}$ s^{-1}. The slow rate of the reaction, as reflected in the small value of k_{cat} as well as the EPR data discussed below, is fully consistent with preequilibrium formation of LCu−S−CuL followed by its slow decomposition to products. In the above mechanism we assume that deprotonation of coordinated water on Cu(II) occurs prior to step (3) and that attack of coordinated hydroxide at phosphate, step (3), is rate-determining (see structures **1a**−**c**) in analogy with findings for [Cu[9]aneN_3Cl_2].[26,27]

EPR Studies. EPR studies were conducted in order to further characterize mechanistic steps and the proposed intermediates of hydrolysis (**1a**−**c**). The EPR spectra of 1 mM ^{63}Cu(tach-Me_3)$^{2+}$ at room temperature and in frozen (77 K) solution in HEPES buffer (pH 7.4) (Figure 4) reveal ^{63}Cu ($I = 3/2$) hyperfine lines characteristic of a monomeric cupric complex.[33,42] The relative values of the double integrals of the spectrum of ^{63}Cu(tach-Me_3)$^{2+}$ in the frozen solution and that of the $CuSO_4$ intensity standard were within 2%, indicating that the EPR signal accounts for all of the copper in the tach-Me_3 sample. These observations, plus the fact that the EPR signal amplitude for the frozen or room-temperature solution was found to be a linear function of concentration in the range 1−10 mM, demonstrate that significant amounts of dimeric species (<3%) are not formed in these solutions. Thus, it is unlikely that a preformed hydroxo-bridged copper dimer[26,27] (e.g., {[Cu(tach-Me_3)]$_2$(μ-OH)$_x$}$^{(4-x)+}$) is the catalyst or catalyst precursor. In contrast, upon addition of 10 mM BNPP, the double integrals of both the frozen and room-temperature solution spectra of 1 mM Cu(tach-Me_3)$^{2+}$ were markedly reduced, by 21 ± 3% and 37 ± 2%, respectively, compared to the spectrum of the Cu(tach-Me_3)$^{2+}$ complex in the absence of BNPP. The appearance and line shape of the spectra in Figure 4 were unchanged, only their intensities reduced, and no new species were observed. These findings strongly suggest that significant amounts of EPR-silent dimeric (or possibly oligomeric) species are formed *only when substrate is present in the solution*. From the value of overall dissociation constant $K_M = 12.3$ mM^2 derived from the kinetic data of Figure 3, we estimate that approximately 44% of the copper is in the dimeric form under the concentration conditions of the EPR experiment, a value that compares favorably with the observed 37% reduction in the EPR signal of the room-temperature solution. Thus, the EPR data support the hypothesis that the substrate binds to monomeric Cu(tach-Me_3)$^{2+}$ (step (1)), enabling a dimer to form (step (2)) and rule out preformation of a hydroxo-bridged copper dimer prior to binding of substrate.

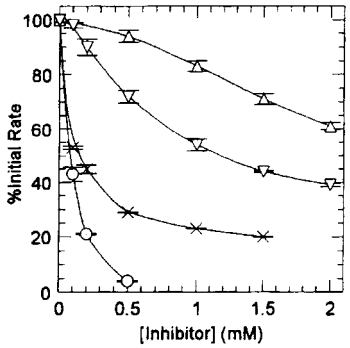

Figure 5. Inhibition of bis(*p*-nitrophenyl) phosphate hydrolysis promoted by Cu(tach-Me_3)$^{2+}$. Each reaction mixture contained 50 mM HEPES, pH 7.2, at 50 °C, 2 mM bis(*p*-nitrophenyl) phosphate, and 1 mM Cu(tach-Me_3)$^{2+}$. The concentration of the inhibitor ranged from 0.1 mM to a maximum of 2 mM. The data are expressed as the percentage of initial rate retained. The computer-generated lines illustrate the trend in the data. Key: △, *p*-nitrophenyl phosphate; ▽, phenyl phosphate; ×, phosphate; ○, pyrophosphate.

Substrate Comparison. The observed first-order rate constants for bis(*p*-nitrophenyl) phosphate, ethyl *p*-nitrophenyl phosphate, and *p*-nitrophenyl phosphate hydrolysis are given in Table 1. Bis(*p*-nitrophenyl) phosphate was hydrolyzed more rapidly than the ethyl derivative, in accord with the greater electron-withdrawing and leaving-group characteristics of the *p*-nitrophenyl group relative to ethyl. The phosphate monoester, *p*-nitrophenyl phosphate, was hydrolyzed much less rapidly than the diesters, consistent with it being a dianion, which is less susceptible to nucleophilic attack than the monoanionic substrates.

Hydrolysis Inhibition. The hydrolysis of bis(*p*-nitrophenyl) phosphate by Cu(tach-Me_3)$^{2+}$ was inhibited by the monoester product of the reaction, *p*-nitrophenyl phosphate. The effects of phenyl phosphate, inorganic phosphate, and pyrophosphate ($P_2O_7^{4-}$) were also studied (Figure 5). The greatest inhibition was seen with pyrophosphate, which is the most basic, and is well-known to bridge metal centers in dimeric complexes.[43,44] The hydrolysis reaction was completely inhibited with the

(42) Pilbrow, J. R. *Transition Ion Electron Paramagnetic Resonance*; Clarendon Press: Oxford, U.K., 1990; pp 624−626.

(43) Ainscough, E. W.; Brodie, A. M.; Ranford, J.; Waters, J.; Murray, K. *Inorg. Chim. Acta* **1992**, *197*, 107.

Table 1. Observed First-Order Rate Constants for the Hydrolysis of Phosphate Esters by [Cu(tach-Me_3)Cl_2][a]

phosphate ester	k_{obs} (s^{-1})[b]
bis(*p*-nitrophenyl) phosphate	$(1.12 \pm 0.02) \times 10^{-5}$
ethyl *p*-nitrophenyl phosphate	$(6.9 \pm 0.4) \times 10^{-7}$
p-nitrophenyl phosphate	$(1.12 \pm 0.06) \times 10^{-8}$

[a] Conditions:1 mM [Cu(tach-Me_3)Cl_2]; 5 mM phosphate ester; pH 7.2; 50 °C. [b] k_{obs} = initial rate/[phosphate ester].

addition of 0.5 equiv of pyrophosphate relative to Cu(tach-Me_3)$^{2+}$. Phosphate was also a potent inhibitor. As the concentration of phosphate was increased, the rate of product formation rapidly deviated from pseudo-first-order behavior, and a faint precipitate was observed, possibly a phosphate complex of Cu(tach-Me_3)$^{2+}$. Phenyl phosphate was found to be a better inhibitor than *p*-nitrophenyl phosphate. The *p*-nitrophenyl group is more electron-withdrawing than phenyl, which suggests that phenyl phosphate would be more basic than *p*-nitrophenyl phosphate and would in turn have a greater affinity Cu(II) center, leading to the observed order of inhibition.

Discussion

This study focuses on the mechanism of action of Cu(tach-Me_3)$^{2+}$ in the hydrolysis of activated phosphate diesters. Copper(II) complexes may catalyze hydrolysis of phosphodiesters, two requirements being that the metal center possess adequate Lewis acidity and open coordination sites. However, beyond these factors, mechanistic studies show that kinetics, proposed intermediate species, and other aspects of Cu(II)-promoted phosphate diester hydrolysis vary considerably. The properties of Cu(tach-Me_3)$^{2+}$ may be compared to [Cu([*n*]aneN_3)X_2] (*n* = 9, 10, 11),[26,27] Cu^{II}(tach-H_3)$^{2+}$,[29] Cu(2,2′-bipyridine)$^{2+}$,[20] and Cu(II) bis(2-benzamidoylmethyl)amine.[25]

The solid-state structure of [Cu(tach-Et_3)$Br_{0.8}Cl_{1.2}$][33] is similar to [Cu([9]aneN_3)Cl_2],[45,46] a substance which is also active in hydrolysis of BNPP. Both present Cu(II) in a five-coordinate, distorted square-pyramidal geometry with an elongated apical nitrogen bond, a result of Jahn−Teller distortion in the d^9 electron configuration. The rate of Cu(tach-Me_3)$^{2+}$-promoted phosphate diester hydrolysis (Table 1) is slightly faster than the rate of Cu([9]aneN_3)$^{2+}$-promoted hydrolysis under comparable conditions.[26] Thus, the observed first-order rate constant for [Cu([9]aneN_3)Cl_2]-promoted hydrolysis of bis(*p*-nitrophenyl) phosphate is 1.3×10^{-6} s^{-1},[26] approximately 8-fold smaller than Cu(tach-Me_3)$^{2+}$ ($k_{obs} = 1.1 \times 10^{-5}$) (Table 1). A similar rate acceleration factor of 9.6 is observed for hydrolysis of ethyl(*p*-nitrophenyl) phosphate by Cu(tach-Me_3)$^{2+}$ (Table 1) compared to Cu([9]aneN_3)$^{2+}$ ($k_{obs} = 7.2 \times 10^{-8}$ s^{-1}).[26] In terms of ligand structure, Cu(tach-H_3)$^{2+}$ most closely resembles Cu(tach-Me_3)$^{2+}$; however, no [Cu(tach-H_3)X_2] complexes have been isolated or structurally characterized for comparison. Under different conditions (pH 8.1 at 25 °C) Fujii and co-workers[29] found $k_{cat} = (2.6 \pm 0.1) \times 10^{-4}$ s^{-1} for the hydrolysis of ethyl 2,4-dinitrophenyl)phosphate by Cu(tach-H_3)$^{2+}$, offering a limited comparison with $k_{cat} = (4.0 \pm 0.4) \times 10^{-4}$ s^{-1} for BNPP hydrolysis by Cu(tach-Me_3)$^{2+}$ at pH 7.2 and 50 °C.

Unique features of the Cu(tach-Me_3)$^{2+}$ system are revealed in the study of solution speciation. In the Cu(tach-H_3)$_3^{2+}$ system, the proposed active solution species is [Cu(tach-H_3)(OH_2)-$(OH)]^+$.[29] In the catalysts based on [Cu([*n*]aneN_3)X_2] (*n* = 9, 10, 11), the solution speciation is believed to be a monomer−dimer mixture of [Cu([*n*]aneN_3)$(OH)]^+$ and [Cu([*n*]aneN_3)(μ-$OH)]_2^{2+}$.[27] These complexes contrast with our assignment of the solution form of Cu(tach-Me_3)$^{2+}$(aq) as [Cu(tach-Me_3)-$(H_2O)_2]^{2+}$.[33] It is not clear why Cu(tach-Me_3)$^{2+}$(aq) does not form a hydroxo species; a tentative explanation is a greater electron-donating ability of tach-Me_3 relative to tach-H_3, which diminishes the Lewis acidity of Cu(II).

Hydrolysis of phosphodiesters by Cu(tach-Me_3)$^{2+}$ exhibits second-order rate dependence on metal complex, to the best of our knowledge a property that is shared by only one other mononuclear Cu(II) complex, Cu(II) bis(2-benzamidoylmethyl)-amine.[25] The kinetics of the Cu(tach-H)$_3^{2+}$ system has been reported as first-order in Cu(II) for the cleavage of ethyl (2,4-dinitrophenyl) phosphate.[29] [Cu([*n*]aneN_3)X_2] (*n* = 9, 10, 11) exhibits $^1/_2$-order dependence on Cu(II), attributed to the dissociation of [Cu([*n*]aneN_3)(μ-OH)]$_2^{2+}$ that is required to generate the active catalyst.[26]

On the basis of the second-order kinetics of Cu(tach-Me_3)$^{2+}$, we have postulated a binuclear intermediate (one of structure types **1a**, **1b**, or **1c**) in the cleavage process. Alkyl phosphates are known to bridge two copper centers through the linkage Cu−O−P−O−Cu, as in [Cu_2(phen)$_2$(ATP)$_2$][47] and [Cu_2(6,6′-($Me_3NCH_2C_2$)$_2$bipy)$(H_2O)_2$(1,3-μ-$PO_3OPh)_2$] $[NO_3]_4$.[22] Support for the assertion that a LCu−S−CuL species forms in the BNPP hydrolysis reaction is derived from analysis of kinetic data (Figure 3) and from EPR studies. EPR studies of the copper complex in the presence and absence of substrate clearly indicate that no measurable amounts of binuclear Cu(tach-Me_3)$^{2+}$ complexes are present in solution in the absence of the substrate, while, in the presence of substrate, a significant decrease in EPR signal intensity is observed, which is in accord with formation of an antiferromagnetically coupled dimeric complex in an amount consistent with the kinetic data. Thus, structure **1b** is an unlikely intermediate because it would not be strongly exchange-coupled. Further EPR experiments and magnetic susceptibility measurements are needed to better define the nature of the putative dimeric species and also those formed in the presence of inhibitors.

To interpret the kinetic data, we have derived and applied a model for hydrolysis incorporating the formation of an LCu−S−CuL intermediate (**1**) in an equilibrium step (eqs 1 and 2) and the breakdown of **1** to products in an irreversible rate-determining step (eq 3). The presence of an LCu−S−CuL species is quantitatively supported by the interpretation of the saturation kinetic data, measured in the reaction of Cu(tach-Me_3)$^{2+}$ with excess BNPP (Figure 3). Unlike Cu[9]aneN_3Cl_2, the onset of saturation was observed at relatively low concentrations of bis(*p*-nitrophenyl) phosphate. The rate of ligand exchange for Cu(II) complexes is greater than that of phosphate ester hydrolysis;[48] thus, our model predicts that the rate-limiting step involves breakdown of the substrate-bridged binuclear complex to products. The excellent fit of eq 7 to the experimental data (Figure 3), as well as the extent of decrease in EPR intensity, described above, is consistent with this proposal. From this analysis, the equilibrium constant for the coordination of bis(*p*-nitrophenyl) phosphate to a single Cu(tach-Me_3)$^{2+}$ is approximately $1/K_M^{1/2}$, or ca. 300 M^{-1}. This value is a geometrical average of K_1 and K_2 from eqs 1 and 2, which assume sequential binding of Cu(tach-Me_3)$^{2+}$ to the substrate.

(44) Herron, N.; Thorn, D.; Harlow, R.; Coulston, G. *J. Am. Chem. Soc.* **1997**, *119*, 7149.
(45) Schwindinger, W.; Fawcett, T.; Lalancette, R.; Potenza, J.; Schugar, H. *Inorg. Chem.* **1980**, *19*, 1379.
(46) Bereman, R.; Churchill, M.; Schaber, P.; Winkler, M. *Inorg. Chem.* **1979**, *18*, 3122−3125.
(47) Sheldrick, G. M. *Angew. Chem., Int. Ed. Engl.* **1981**, *20*, 460−461.
(48) Wilkins, R. *Kinetics and Mechanism of Reactions of Transition Metal Complexes*, 2nd ed.; VCH: Weinheim, Germany, 1991.

Values of 20 and 15 M^{-1} have been observed for saturation of the hydrolysis of ethyl *p*-nitrophenyl phosphate, by Cu(2,2′-bipyridine)[20] and Cu[9]aneN_3Cl_2,[26] respectively. Ethyl *p*-nitrophenyl phosphate is presumably a stronger base than BNPP, and much higher values of K_M would be expected on this basis. The markedly higher affinity of Cu(tach-Me_3)$^{2+}$ for the phosphate diester suggests factors such as greater Lewis acidity of Cu(tach-Me_3)$^{2+}$ relative to Cu(2,2′-bipyridine)$^{2+}$ or Cu[9]aneN_3-Cl_2 are operating and requires further investigation.

We find that phosphates inhibit BNPP cleavage by Cu(tach-Me_3)$^{2+}$ with a stoichiometry that is consistent with formation of a phosphate-bridged dimer (Figure 5). Thus, hydrolysis of bis(*p*-nitrophenyl) phosphate was completely inhibited by 0.5 mol equiv of pyrophosphate relative to Cu(tach-Me_3)$^{2+}$, suggesting that pyrophosphate bridges two Cu(tach-Me_3)$^{2+}$ complexes nonreversibly. Pyrophosphates are known to bridge two Cu(II) or VO^{2+} centers.[43,44] The order of effectiveness of inhibition by the phosphates is *p*-nitrophenyl phosphate < phenyl phosphate < phosphate < pyrophosphate, which parallels their predicted basicity[49] and presumed affinity for the Cu(II) center.

The source of the nucleophile that cleaves *p*-nitrophenolate from phosphorus and the mechanism of its attack are as yet unknown. Studies suggest that coordinated hydroxide is the nucleophile for some inert[8,9] and labile[20,50] metal complexes; however, a nucleophile originating from outside the metal coordination sphere cannot be excluded at present. [Cu(tach-Me_3)]$^{2+}$ may cleave *p*-nitrophenolate (RO^-) from phosphorus by a concerted process (i.e., the addition of hydroxide and RO−P cleavage are simultaneous) or by an associative process, with stepwise addition of HO^- followed by RO^- departure. Both concerted[50] and associative mechanisms[8,9] have been proposed. It is presumed that the transition state structure(s) resemble the intermediates depicted by **1**, in which the two trans-disposed bonds to P (RO−P−OH) are involved in the bond-formation and bond-dissociation processes. Further studies will be necessary to determine if an associative or concerted pathway dominates.

Conclusion

Cu(tach-Me_3)$^{2+}$-promoted hydrolysis of phosphodiesters exhibits several interesting mechanistic features whose origins are not fully understood. The dimeric intermediate that we postulate has been proposed in the Cu(II)−bis(2-benzamidoylmethyl)-amine system but is in sharp contrast to two very similar systems, Cu(II)−tach-H_3 and [Cu([*n*]aneN_3)X_2] ($n = 9, 10, 11$). The fact that these two systems themselves differ considerably in kinetic behavior further underscores subtle differences in the mechanism of phosphate ester hydrolysis by Cu(II). N-alkylation of the amines on triaminocyclohexane may increase the steric bulk around the copper atom, inhibiting the dimer formation which [Cu([*n*]aneN_3)]$^{2+}$(aq) exhibit. It may also be postulated that a greater electron-donating ability of tach-Me_3 prevents Cu-(tach-Me_3)$^{2+}$(aq) from hydrolysis to a hydroxo species, in contrast to Cu(tach-H_3)$^{2+}$. It is clear that further studies are necessary to elucidate the nature of metal complex intermediates and nucleophiles in this process.

Potential biological applications of Cu(tach-Me_3)$^{2+}$ are of interest. The intermediates **1** proposed herein resemble those of the purple acid phosphatases[19] and those for the hydrolysis of DNA at the exonuclease site of DNA polymerase I.[51,52] Cu-(II) complexes of [9]aneN_3 and tach-H_3 are known to cleave plasmid DNA.[36,53] Further studies of the action of Cu(tach-Me_3)$^{2+}$ on biological macromolecules, as well as its effects on cultured tumor cells, are in progress.

Acknowledgment. The authors thank A. C. Hengge and J. N. Burstyn for helpful discussions. N.D.C. thanks the NIH for support (Grant No. R37-GM20194).

IC000830D

(49) Wulfsberg, G. *Principles of Descriptive Inorganic Chemistry*; Univ Sci Bks: Mill Valley, CA, 1991; p 34 ff.
(50) Deal, K.; Hengge, A.; Burstyn, J. *J. Am. Chem. Soc.* **1996**, *118*, 1713−1718.
(51) Beese, L.; Steitz, T. *EMBO J.* **1991**, *10*, 25−33.
(52) Freemont, P.; Friedman, J.; Beese, L.; Sanderson, M.; Steitz, T. *Proc. Natl. Acad. Sci. U.S.A.* **1988**, *85*, 8924−8928.
(53) Hegg, E. L.; Burstyn, J. N. *Inorg. Chem.* **1996**, *35*, 7474−7481.